J Fluoresc (2010) 20:1225–1231
DOI 10.1007/s10895-010-0672-7

ORIGINAL PAPER

Erythrocyte Protoporphyrin Fluorescence as a Biomarker for Monitoring Antiangiogenic Cancer Therapy

Flávia Gomes de Góes Rocha · Karen Cristina Barbosa Chaves · Cinthia Zanini Gomes · Camila Barricheli Campanharo · Lilia Coronato Courrol · Nestor Schor · Maria Helena Bellini

Received: 2 February 2010 / Accepted: 4 May 2010 / Published online: 18 May 2010

Abstract Renal cell carcinoma (RCC) remains one of the greatest challenges of urological oncology and is the third leading cause of death in genitourinary cancers. RCCs are highly vascularized and are amenable to antiangiogenic therapy. Endostatin (ES) is a fragment of collagen XVIII that possesses antiangiogenic activity. In this study, we examined the potential of erythrocyte PpIX fluorescence spectroscopy for monitoring the efficacy of antiangiogenic therapy in metastatic renal cell carcinoma (mRCC), using an orthotopic metastatic mouse model. Balb/C-bearing Renca cells were treated with NIH/3T3-LendSN cells. Lung weight, nodule area, microvascular area (MVA), and erythrocyte PpIX fluorescence were evaluated. Emission spectra were obtained by exciting the samples at 405 nm. There was a significant decrease in lung wet weight, lung nodule area and MVA in the treated group compared to the control group ($P<0.001$). Significant differences in autofluorescence shape were observed in the 620–650 nm spectral region. The most intense fluorescence peak was observed at ~632 nm. The autofluorescence of the control samples was about 53% higher than that of normal blood ($P<0.05$). In the group treated with ES, the autofluorescence was about 54% lower than in the control group ($P<0.05$). Fluorescence intensity was positively correlated with the nodule area ($R^2=0.8859$; $P<0.001$) and MVA ($R^2=0.9431$; $P<0.001$) in the ES-treated group. These results demonstrate that the spectroscopic analysis method allows a selective detection of tumor masses. This preliminary study suggests that PpIX fluorescence may be useful as a biomarker for antiangiogenic cancer therapy.

Keywords RCC · Endostatin · Porphyrin · Fluorescence · Animal model · Metastasis

F. G. de Góes Rocha · K. C. B. Chaves · C. Z. Gomes · M. H. Bellini (✉)
Centro de Biotecnologia, IPEN/CNEN-SP,
São Paulo, SP, Brazil
e-mail: mbmarumo@ipen.br

F. G. de Góes Rocha · K. C. B. Chaves · C. B. Campanharo · N. Schor · M. H. Bellini
Disciplina de Nefrologia, Departamento de Medicina, UNIFESP,
São Paulo, SP, Brazil

L. C. Courrol
Departamento de Ciências Exatas e da Terra, UNIFESP,
São Paulo, SP, Brazil

L. C. Courrol
Centro de Lasers e Aplicações, IPEN/CNEN-SP,
São Paulo, SP, Brazil

Introduction

Angiogenesis is a physiological process involving the growth of new blood vessels from pre-existing vessels. Unregulated angiogenesis, however, is a crucial step in tumor growth and progression. Its quantification by microvessel counting is of prognostic value in several types of malignancies [1].

RCC represents about 85% of the newly diagnosed renal cell cancers, which occur at an estimated rate of 4.4–11.1 cases per 100,000 people per year [2–4].

Surgery may be curative when patients present with localized disease. However, many patients who are initially resected eventually relapse, and the prognosis in these cases is poor. In fact, among patients choosing excision of a localized RCC, approximately 20% will subsequently experience recurrence of the disease. RCC metastases to the lungs are the most frequent, with prevalence rates as high as 72% and 76% in autopsy studies [5, 6].

RCC is a highly vascularized tumor. It secretes several growth factors, such as vascular endothelial growth factor (VEGF), platelet-derived growth factor (PDGF), and soluble vascular endothelial growth factor receptor 2 (VEGFR2). Elevated serum levels of growth factors and imaging techniques have been used to monitor patients after surgery [7]. RCC is amenable to antiangiogenic therapy, as evidenced by the recent approval of new antiangiogenic agents that target the VEGF/VEGF receptor pathway [8, 9]. Along with these exciting new therapeutic agents, including ES gene therapy, comes the challenge of detecting useful biomarkers to monitor patients receiving these therapies. Although many patients benefit from antiangiogenic therapies, it is not always possible to achieve stabilization of the disease. Thus, the development of noninvasive biomarkers of disease response and relapse is a crucial objective to aid in the management of these patients [10].

ES is a 20-kDa fragment cleaved from a collagen XVIII COOH terminus that inhibits endothelial cell proliferation, migration, invasion, and tube formation, and has dramatically reduced tumor growth and metastasis in several mouse models, with no serious side effects observed [11–15]. In a previous study performed by our group, subcutaneous injection of ES-transduced cells resulted in significant anti-tumor effects in a murine model of renal carcinoma. Histological analysis of treated tumors showed decreased microvascular density, massive necrosis and foci of apoptotic cells, which were associated with leukocyte infiltration [8].

Fluorescence spectroscopy is currently one of the most widely used spectroscopic techniques in the fields of biochemistry and molecular biophysics. Natural tissue fluorophores such as NAD-(P)H and FAD, structural proteins such as collagen, elastin, and their crosslinks, and the aromatic amino acids tryptophan, tyrosine, phenylalanine and porphyrins display characteristic excitation wavelengths with an associated characteristic emission [16, 17]. Biophysical changes that accompany dysplastic progression often lead to alterations in the optical characteristics of tissues. Optical technologies sensitive to these alterations can lead to the development of quantitative, noninvasive, real-time diagnostic tools [16].

Protoporphyrin, a porphyrin derivative, is the intermediate metabolic precursor of the heme molecule. The insertion of ferrous iron into protoporphyrin IX (catalyzed by the enzyme ferrochelatase) is the last step in heme biosynthesis. In erythrocytes, a small portion of protoporphyrin normally escapes this metabolizing process and can be found as free erythrocyte protoporphyrin IX (FEP) or as zinc protoporphyrin (ZP), an alternative chelate to heme [17]. Measurement of both forms has potential as a screening test for diseases. Protoporphyrin IX (PpIX) accumulates in cancerous tissues as a consequence of tumor-specific metabolic alterations. Several studies have been performed to define the potential of autofluorescence for cancer diagnosis [18–20].

In a previous study [20], our group demonstrated the autofluorescence of blood PpIX in xenoimplanted SCID mice and an increase in fluorescence intensity at ~635 nm as a function of growth of the subcutaneous tumor mass. In another work, tumor-bearing kidneys in different progression stages were analyzed by ex-vivo spectroscopy, and a nice correlation between the growth of the tumor mass and fluorescence intensity was found [21].

The aim of this work was to evaluate the potential of fluorescence spectroscopy for monitoring antiangiogenic cancer therapy.

Materials and methods

Cell lines

NIH/3T3-LendSN-clone 3 was utilized for endostatin expressing. The cells were maintained in DMEM with high glucose content (4.5 g/l at 25 mM), and supplemented with 100 U/ml penicillin, 50 mg/ml streptomycin, and 10% fetal bovine serum (Life Technologies). The ES level produced by NIH/3T3-LendSN was 1.36 μg/mL [8].

Renca, a murine RCC line of spontaneous origin in a BALB/c mouse was kindly donated by Dr Isaiah Fidler D. V.M., Ph.D. (from The University of Texas M. D. Anderson Cancer Center, USA). The cells were maintained in RPMI supplemented with 10% fetal bovine serum (Life Technologies) buffered with fresh 2 mM L-glutamine (Life Technologies), 100 U/ml penicillin, and 100 mg/ml streptomycin.

Both cell lines were maintained in a humid chamber at 37°C in an atmosphere containing 5% CO2.

Animals

Male Balb/C mice (10–12 weeks old) were obtained from the Animal Facility of IPEN/CNEN-SP, São Paulo, Brazil. They were kept in a pathogen-free isolator unit, and food and water were autoclaved. All animals were maintained on a daily 12-hr light/12-hr dark cycle. Twenty-five mice were used in the experiment (Normal group - N=5; Control group-N=10; ES-treated group - N=10).

Orthotopic RCC tumor model

The experimental protocol was approved by the Animal Experimentation Ethics Committee.

Mice were anesthetized by subcutaneous injection with Ketamine and Xylazine, 100 mg/kg and 10 mg/kg body

weight, respectively. The left kidney was exteriorized via flank incision, and 10 μl of Renca cells were inoculated (1×10^5 cells/animal) into the renal subcapsular space, using a Hamilton syringe with a 27 gauge needle. The kidney was then returned, the peritoneum sutured, and the incision closed using surgical clips.

Nephrectomy

The left kidney was removed by unilateral nephrectomy 7 days after Renca cells inoculation. The animals were randomly divided into two groups of 10 mice each: one of them was the control, and the other received a subcutaneous inoculation of 3×10^6 NIH/3T3-LendSN cells (ES production level = 1.36 μg/mL).

Five normal mice were used as lung and erythrocyte donors. Ten days later, the animals were killed and exsanguinated.

Blood collection and histological analysis of the lung

At the end of the experiment, the animals were sacrificed following the guidelines for euthanasia of the American Veterinarian Medical Association. A total of 500 μL of blood were collected from each animal and centrifuged at 3,000 rpm for 15 min. The formed elements were used for porphyrin extraction.

The lung was excised, washed in PBS, fixed in 10% PBS-buffered formalin for 24 h, and then routinely processed for paraffin-embedding. Histological analysis was performed in 4 μm sections stained with hematoxylin and eosin.

Assessment of tumor and vascular areas in the lungs from both control and treated animals was performed by morphometry. Images were collected at a lower magnification (20×) using a Nikon Eclypse E600 microscope, in at least 20 independent fields. The vascular and nodule areas were quantified as follows: grids were projected on random fields of lung sections at a 20× magnification, and the number of grid intersections overlaying stained vessels and nodules was counted. Data were expressed in pixels as the relative area of vessels and nodules within the metastatic lung, considering the images in 1280×1024 pixels, and each pixel representing 0.32 μm.

Porphyrin extraction

Three volumes of analytical-grade acetone were added to the 250 μL of erythrocytes, thoroughly mixed, and centrifuged at 3,000 rpm for 15 min. The mixture was then centrifuged at 4,000 rpm for 15 min. The clear supernatant was transferred to a clean tube and maintained at 4°C until spectrofluorimetric analysis.

ELISA analysis

ES was measured in tissue homogenates from lungs of animals subjected to the different treatments, using a Mouse Endostatin ELISA Kit (USCN Life Science & Technology Company, Double Lake, MO), according to the manufacturer's instructions. The endostatin concentrations were assayed at least in triplicate, and the reproducibility of the assay was confirmed.

Fluorescent spectral analyses

The samples were excited at 420 nm and analyzed with a 1-mm path length in a Jobin Yvon (Longjumeau, France) Fluorolog-3 spectrometer with front-face collection geometry and a 0.2-nm resolution. The entrance and exit slits were adjusted respectively at 5 and 2 mm.

Statistical analysis

The results are presented as means ± SE. Single comparisons of the mean values were performed by Student's *t* test. Multiple comparisons of mean values were performed using one-way ANOVA followed by Bonferroni's test, using GraphPad Prism version 4.0 for Windows® (GraphPad® Software, San Diego, CA, USA), http://www.graphpad.com. A probability (*P*) value of less than 0.05 was considered statistically significant.

Results

At the end of the experiment, the ES serum levels of the normal and of the ES-treated group were measured. ES serum levels were higher in the control group than in healthy mice ($P<0.05$). As shown in Fig. 1a, subcutaneous inoculation of NIH/3T3-LendSN cells (ES group) resulted in a 2.75-fold increase of the circulating ES levels (normal vs ES $P<0.001$).

To quantify the lung tumor burden, the lung of each animal was isolated and immediately weighed (wet weight). The mean lung wet weight for the groups studied was: control group = 0.78±0.08; ES-treated group = 0.28±0.01. As expected, the lung wet weight was increased in the control group compared to normal animals (0.18±0.01 $P<0.001$). In the ES-treated group, there was a significant decrease of lung weight compared to the control group ($P<0.001$) Fig. 1b.

Histological and morphometric analysis

Booming proliferation of tumor cells and severe destruction of lung tissue were observed by HE staining in the control

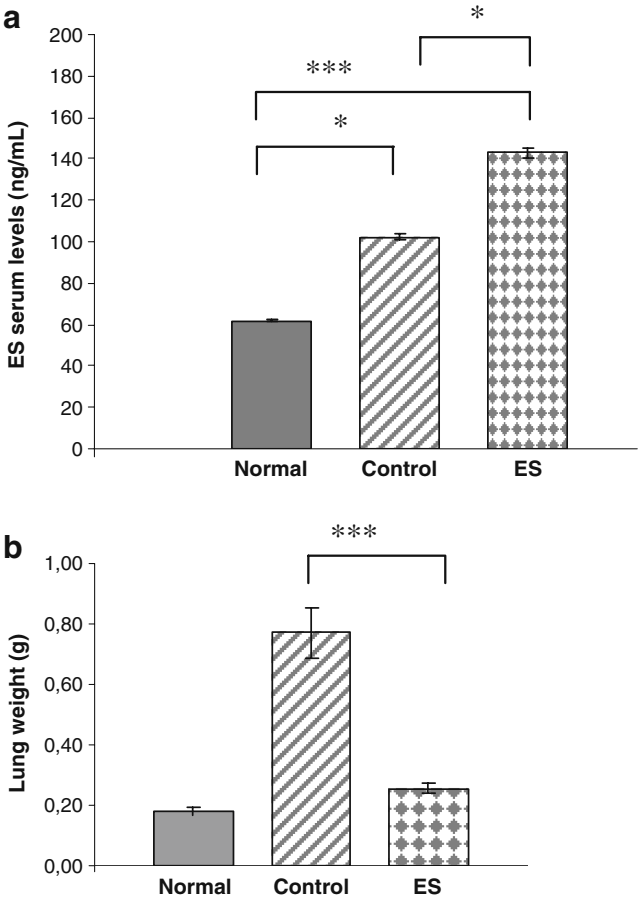

Fig. 1 Orthotopic metastatic animal model of RCC. **a** ES serum levels of normal and experimental groups (normal vs control *P< 0.05; normal vs ES group ***P<0.001); **b** Mean lung wet weight of normal and experimental groups: lung weight of ES-treated group was significantly lower than of control group (***P<0.001) (ANOVA)

group, whereas in the animals treated with ES the lung tissue was better preserved (Fig. 2a and b).

Metastatic foci in lung parenchyma were significantly smaller in the treated groups (P<0.001) (Fig. 3a).

Microvascular morphometry of the tumors showed that, in the treated groups, the microvascular area (MVA) was significantly decreased (P<0.001) (Fig. 3b), demonstrating the efficiency of ES for antiangiogenic cancer therapy.

Fluorescence analyses

The samples were excited at 420 nm, and emission was collected between 600 nm and 730 nm. The spectrum consisted of two main peaks around 632 and 690 nm, respectively. The most intense fluorescence peak was observed at ~632 nm. The PpIX autofluorescence of the control samples was about 53% higher than that of normal blood (P<0.05). In the ES-treated group, the autofluorescence was about 54% lower than in the control group (P<0.05). The reduction in autofluorescence produced by the ES treatment resulted in values that did not differ significantly from the normal group (Fig. 4).

Although the number of samples was too small to perform rigorous statistical analyses, the fluorescence intensity ratio was positively correlated with the nodule area (R^2=0.8859; P<0.001) and MVA (R^2=0.9431; P< 0.001) in the ES-treated group (Fig. 5a and b).

Discussion

A variety of antiangiogenic agents are currently available for the treatment of many types of cancer and there is an urgent need for reliable, sensitive, and quantitative in vivo measurement techniques for evaluating the antiangiogenic therapies.

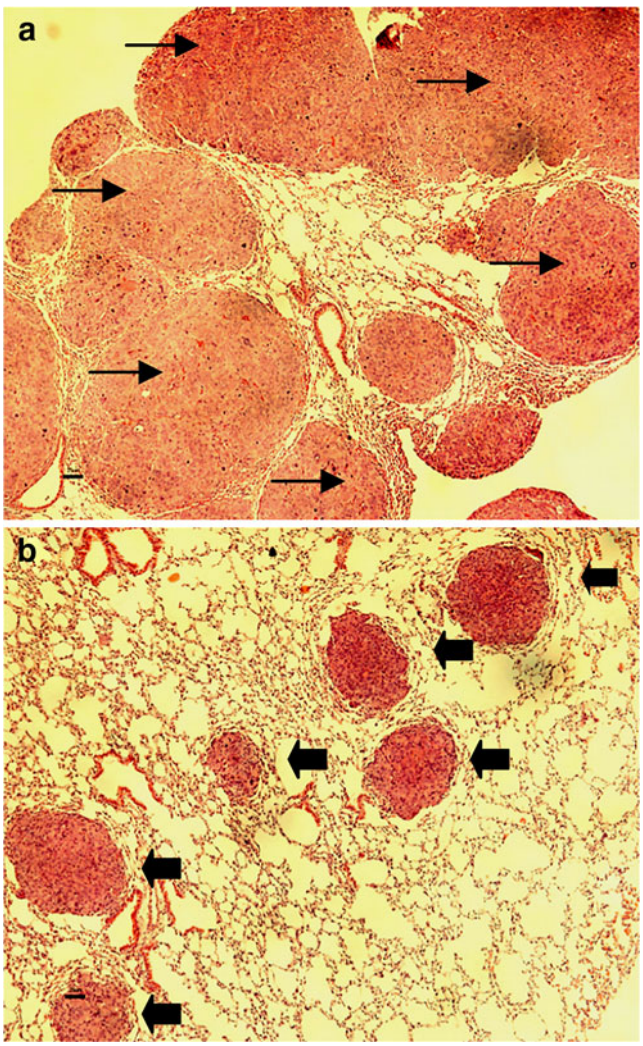

Fig. 2 Microscopic view of the HE-stained lung tissues (a,b). **a** Control group: numerous large tumor nodules almost completely replacing normal parenchyma (arrows); **b** ES-treated group: small tumor nodules seen within the lung tissue (arrows) Magnification (40×)

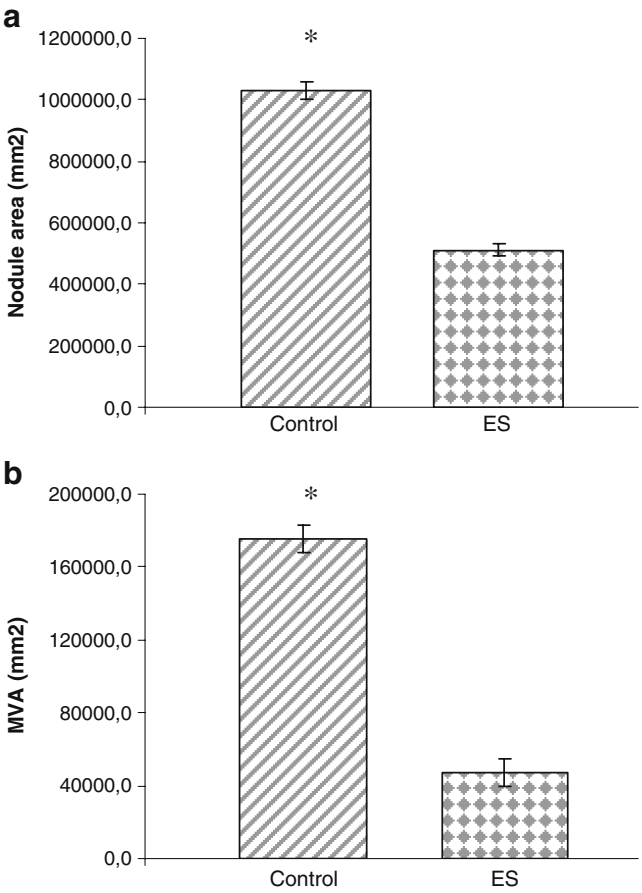

Fig. 3 Effect of ES treatment on mRCC. **a** Lung nodule area: ES-treated group with nodule area significantly smaller than in the control group (*P<0.001); **b** MVA: Microvascular density significantly decreased in the ES-treated group compared to control (*P<0.001)

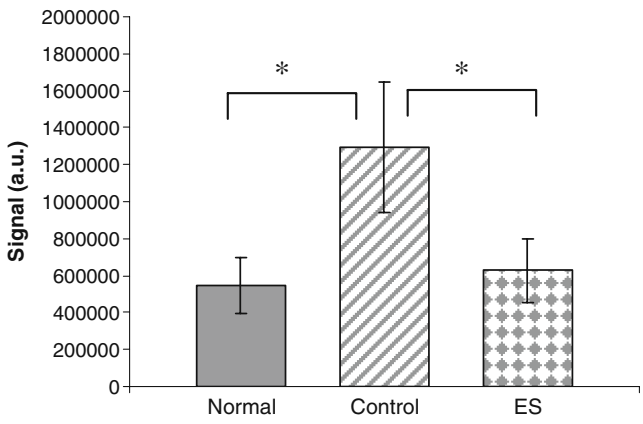

Fig. 4 Erythrocyte PpIX fluorescence intensity in blood samples from the normal, control and ES-treated groups. There is a significant difference between normal and control (*P<0.05). ES treatment produced a significant reduction in erythrocyte PpIX fluorescence. (*P<0.05). The ES-treated group did not differ significantly from the normal group (ANOVA)

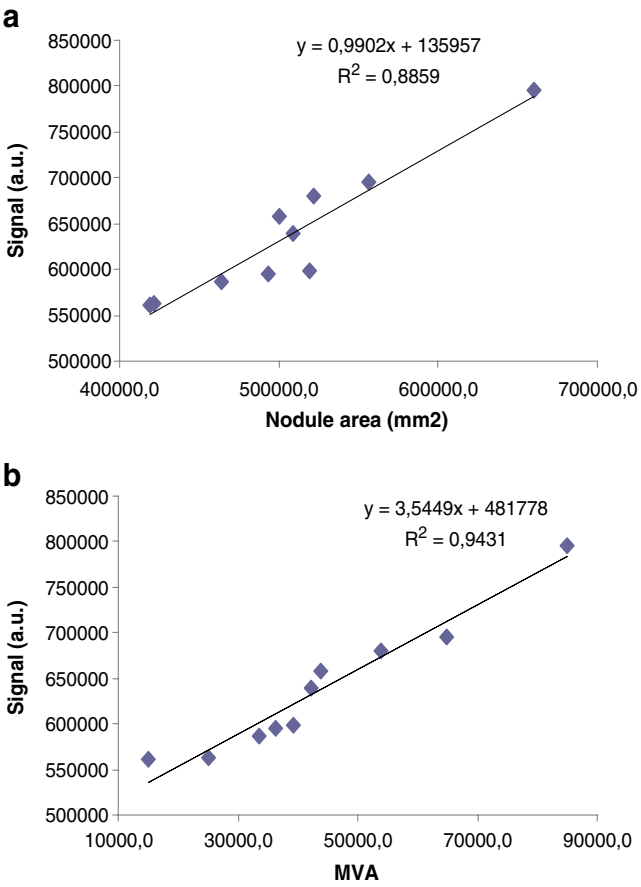

Fig. 5 Correlation analysis. **a** Nodule area vs erythrocyte PpIX fluorescence; **b** MVA vs erythrocyte PpIX fluorescence (P<0.001 for both)

In this study, we used a Balb/C orthotopic metastatic model of RCC to evaluate the efficacy of ES gene therapy and also the potential of fluorescence spectroscopy for monitoring the antiantiogenic therapy.

In a previous study [21], our group demonstrated the autofluorescence of blood PpIX in a primary tumor model of RCC and the increase in fluorescence intensity at ~635 nm as a function of growth of the subcutaneous renal tumor mass. In the present work, we demonstrated that distant RCC metastases also show a distinct and enhanced fluorescence band (around 632 nm) produced by protoporphyrin. An abnormal PpIX metabolism has been observed in blood, plasma, serum and other tissues of cancer patients, indicating that cancer cells accumulate substantially more PpIX than the normal cells and tissues [22–25]. The enhanced fluorescence of endogenous porphyrins in cancerous tissues is assumed to be a consequence of the tumor-specific metabolic alterations which can be caused by tumor hypervascularity [26, 27].

In the ES-treated group, the lung tumor burden was significantly inhibited. Our morphometric data show that sustained release of ES by NIH/3T3-LendSN-clone 3

promoted a significant reduction in nodule area and MVA. Previous studies have demonstrated that the mean microvessel diameter increases as the cancer stage progresses [28]. The reduction of tumor vessels and, consequently, of tumor volume is evidence that the antiangiogenic therapy was effective. The PpIX levels in the endogenous erythrocytes of the ES-treated group were 54% lower than in controls, indicating that PpIX fluorescence could be used to monitor a mRCC antiangiogenic treatment. In human colorectal cancers, PpIX fluorescence was used to discriminate metastatically involved lymph nodes from all other palpable nodes. Moreover, the PpIX fluorescence level was also reduced in primary tumors after neoadjuvant treatment [27].

Microvessel density is nowadays widely accepted as an indicator of disease severity across a broad range of cancers, including melanomas, genitourinary, non-small cell lung, and even hematological cancers [28, 29]. Previous studies have compared microvessel density with patient survival in RCC. Other studies have demonstrated an inverse relationship between microvessel density and RCC prognosis [10]. In this study, we demonstrated that the erythrocyte autofluorescence is positively correlated with nodule area and MVA, indicating that fluorescence spectroscopy may be useful as a biomarker for antiangiogenic cancer therapy.

Conclusions

The reduction of lung nodule area and MVA demonstrates that mRCC is responsive to ES therapy. There was a good correlation between the histological and morphometric diagnosis with the fluorescence spectroscopy data, indicating that this technique may be helpful in the fight against cancer.

Acknowledgements This study was supported by FAPESP [Process number: 07/54253-6] and CNPq [Process number: 481888/2008].

References

1. Tonini T, Rossi F, Claudio PP (2003) Molecular basis of angiogenesis and cancer. Oncogene 22:6549–6556
2. Gupta K, Miller JD, Li JZ, Russell MW, Charbonneau C (2008) Epidemiologic and socioeconomic burden of metastatic renal cell carcinoma (mRCC): a literature review. Cancer Treat Rev 34:193–205
3. Chow WH, Devesa SS, Warren JL, Fraumeni JF Jr (1999) Rising incidence of renal cell cancer in the United States. JAMA 281:1628–1631
4. Hollingsworth JM, Miller DC, Daignault S, Hollenbeck BK (2007) Five-year survival after surgical treatment for kidney cancer: a population–based competing risk analysis. Cancer 109:1763–1768
5. Assouad J, Petcova B, Berna P, Dujon A, Foucault C, Riquet M (2007) Renal cell carcinoma metastases surgery: pathologic findings and prognostic factors. Ann Thorac Surg 84(4):1114–1120
6. Weiss L, Harlos JP, Torhost J, Gunthard B, Hartveit F, Svendsen E, Huang WL, Grundmann E, Eder M, Zwicknagl M, Cochrane HR, Stock D, Wright C, Horne CHW (1988) Metastatic patterns of renal carcinoma: an analysis of 687 necropsies. J Cancer Res Clin Oncol 114:605–612
7. Saitoh H (1981) Distant metastasis of renal adenocarcinoma. Cancer 48:1487–1491
8. Coutinho EL, Andrade LNS, Chammas R, Morganti L, Schor N, Bellini MH (2007) Anti-tumor effect of endostatin mediated by retroviral gene transfer in mice bearing renal cell carcinoma. FASEB J 21:3153–3161
9. Kerbel R, Folkman J (2002) Clinical translation of angiogenesis inhibitors. Nat Rev Cancer 2:727–739
10. Martin-Padura I, Bertolini F (2009) Circulating endothelial cells as biomarkers for angiogenesis in tumor progression. Front Biosci (Schol Ed) 1:304–318
11. Folkman J (2004) Endogenous angiogenesis inhibitors. APMIS 112:496–507
12. Boehm T, Folkman J, Browder T, O'Relly MS (1997) Antiangiogenic therapy of experimental cancer does not induce acquired drug resistance. Nature 390:404–407
13. O'Reilly MS, Boehm T, Shing Y, Fukai N, Vasios G, Lane WS, Flynn E, Birkhead JR, Olsen BR, Folkman J (1997) Endostatin: an endogenous inhibitor of angiogenesis and tumor growth. Cell 88:277–285
14. Kirsch M, Schackert G, Black PM (2000) Angiogenesis, metastasis, and endogenous inhibition. J Neuro-oncology 50:173–180
15. Te Velde EA, Vogten JM, Gebbink MFGB, Van Gorp JM, Voest EE, Rinkes IHMB (2002) Enhanced antitumour efficacy by combining conventional chemotherapy with angiostatin or endostatin in a liver metastasis model. Br J Surg 89:1302–1309
16. Schantz SP, Savage HE, Sacks P, Alfano RR (1997) Native cellular fluorescence and its application to cancer prevention. Environ Health Perspect 105(Suppl 4):941
17. Ramanujam N (2000) Fluorescence spectroscopy of neoplastic and non-neoplastic tissues. Neoplasia 2(1–2):89–117
18. Chang KS, Ina P, Marin N, Follen M, Richards-Kortum R (2005) Fluorescence spectroscopy as a diagnostic tool for detecting cervical pre-cancer. Gynecol Oncol 99:S61–S63
19. Vogeser M, Jacob K, Zachoval R (2000) Erythrocyte protoporphyrins in hepatitis C viral infection. Clin Biochem 33(5):387–391
20. Courrol LC, Silva FRO, Coutinho EL, Piccoli MF, Mansano RD, Vieira ND, Schor N, Bellini MH (2007) Study of blood porphyrin spectral profile for diagnosis of tumor progression. J Fluoresc 17 (3):289–292
21. Bellini MH, Coutinho EL, Courrol LC, Silva FRO, Vieira ND, Schor N (2008) Correlation between autofluorescence intensity and tumor area in mice bearing renal cell carcinoma. J Fluoresc 18 (6):1163–1168
22. Kusunoki Y, Imamura F, Uda H, Mano M, Horai T (2000) Early detection of lung cancer with laser-induced fluorescence endoscopy and spectrofluorometry. Chest 118:1776–1782
23. Tsai TM, Hong RL, Tsai JC (2004) Effect of 5-aminolevulinic acid-mediated photodynamic therapy on MCF-7 and MCF-7/ADR cells. Lasers Surg Med 34:64–72

24. Heyerdahl H, Wang I, Liu DL, Berg R, Andersson-Engels S, Peng Q, Moan J, Svanberg S, Svanberg K (1997) Pharmacokinetic studies on 5-aminolevulinic acid-induced protoporphyrin IX, accumulation in tumors and normal tissues. Cancer Lett 112:225–231
25. Malik Z, Kostenich G, Roitman L, Ehrenberg B, Orenstein A (1995) Topical application of 5-aminolevulinic acid, DMSO and EDTA: protoporphyrin IX accumulation in skin and tumors of mice. J Photochem Photobiol B 28:213–218
26. Van Der Breggen EWJ, Rem AI, Cristian MM, Yang CJ, Calhoun KH, Sterenborg HJCM, Motamedi M (1996) Spectroscopic detection of oral and skin tissue transformation in a model for squamous cell carcinoma: autofluorescence versus systemic aminolevulinic acid-induced fluorescence. IEEE J Sel Top Quantum Electron 2:997–1007
27. Moesta KT, Ebert B, Handke T, Nolte D, Nowak C, Haensch WE, Pandey RK, Dougherty TJ, Rinneberg H, Schlag PM (2001) Protoporphyrin IX occurs naturally in colorectal cancers and their metastases. Cancer Res 61:991–999
28. Tsuji T, Sasaki Y, Tanaka M, Hanabata N, Hada R, Munakata A (2002) Microvessel morphology and vascular endothelial growth factor expression in human colonic carcinoma with or without metastasis. Lab Invest 82:555–562
29. Hlatky L, Hahnfeldt P, Folkman J (2002) Clinical application of antiangiogenic therapy: microvessel density, what it does and doesn't tell us. J Natl Cancer Inst 94:883–893